

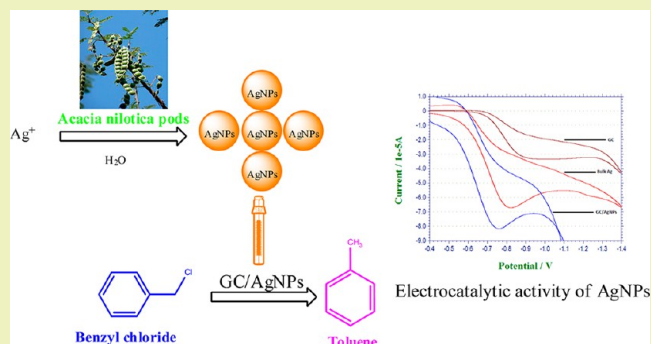
Electrocatalytic Reduction of Benzyl Chloride by Green Synthesized Silver Nanoparticles Using Pod Extract of *Acacia nilotica*

Thomas Nesakumar Jebakumar Immanuel Edison and Mathur Gopalakrishnan Sethuraman*

Department of Chemistry, Gandhigram Rural Institute – Deemed University, Gandhigram 624 302, Dindigul District, Tamil Nadu, India

ABSTRACT: The present work describes the eco-friendly synthesis of silver nanoparticles using pod extract of *Acacia nilotica*. The effect of concentration and effect of pH were studied on the synthesis of silver nanoparticles (AgNPs). The formation of AgNPs was analyzed by visual observation and UV–vis spectrophotometer. Further, the stable AgNPs were characterized by FT-IR, DLS (dynamic light scattering) with zeta potential analysis, and HR-TEM (high resolution-transmission electron microscopy) with EDS (energy dispersive spectrum) analysis. The phytoconstituents present in the extract such as gallic acid, ellagic acid, epicatechin, and rutin are responsible for reduction and protection of Ag^+ and AgNPs, which is evident from FT-IR studies. The studies have revealed that it is possible to control the size of AgNPs by fine-tuning of pH of the reaction medium. The HR-TEM images showed that the synthesized stable AgNPs are approximately 20–30 nm in size with distorted spherical shapes. Further, the electrocatalytic activity of AgNPs on the reduction of benzyl chloride was studied and compared with bulk silver and inert glassy carbon electrode by cyclic voltammetry. The synthesized AgNPs were found to show greater electrocatalytic activity in the reduction of benzyl chloride compared to that of bulk silver as studied from cyclic voltammetry.

KEYWORDS: *Phytosynthesis, Acacia nilotica pods, Silver nanoparticles, Electrocatalyst, Benzyl chloride*



■ INTRODUCTION

Nanoscience and technology has attracted the attention of scientists all over the world, especially in the areas of medicine, materials, energy, catalysis, and sensors, because of the striking difference in physical, chemical, and optical characteristics compared to the bulk materials.^{1–3} The properties of metal nanoparticles strongly depend upon size, shape, stabilizers, and medium.^{4–6} Nanoparticles are synthesized by various methods such as physical vapor deposition, chemical vapor deposition, sol–gel method, microwave synthesis, ultrasonication method, electrochemical method, and reduction of metal ions.^{7–13} Among these methods, colloidal metal nanoparticles with various morphologies are synthesized by the reduction of metal ions using reducing agents. In this method, the addition of a stabilizing agent or capping agent is important because of the fact that synthesized nanoparticles are vulnerable to oxidation in the reaction environment and also in air. The chemicals used for the synthesis and protection of nanoparticles are often toxic, costly, and nonecofriendly. Nowadays nanomaterials, viz., metal nanoparticles, metal oxides, and metal sulphides, are synthesized by bioreduction methods using plant extracts, fungi, microorganisms and green algae as reducing sources.^{14–21} The green methods of synthesis of nanoparticles have advantages such as low cost and eco-friendliness, and usually they give rise to stable nanoparticles.

Acacia nilotica belongs to the Leguminosae family, and the pods contain the phytoconstituents such as gallic acid, ellagic acid, epicatechin, and rutin.²² The chemical structure of phytoconstituents present in the *A. nilotica* extract are shown in Figure 1

In the present work, silver nanoparticles (AgNPs) were synthesized using the aqueous extract of *A. nilotica* pods. The effects of concentration of the extract as well as the effect of pH at various time intervals were studied by visual observation and UV–vis spectrophotometer. The stable AgNPs were further characterized by FT-IR, DLS with zeta potential analysis, and HR-TEM with EDS analysis. Moreover the electrocatalytic activity of AgNPs on the reduction of benzyl chloride was tested using cyclic voltammetry.

■ MATERIALS AND METHODS

Preparation of Extract. From the *A. nilotica* pods, collected from the campus of Gandhigram Rural Institute, Dindigul Dt, Tamil Nadu, India, seeds were completely removed, cleaned, dried, and ground well. About 5 g of the crushed pods was extracted with 100 mL of pure MilliQ water at 80 °C for 30 min, and the extract was filtered using Whatmann filter paper No. 2. The clear filtrate was used for the synthesis of AgNPs.

Received: June 13, 2013

Revised: July 23, 2013

Published: July 28, 2013

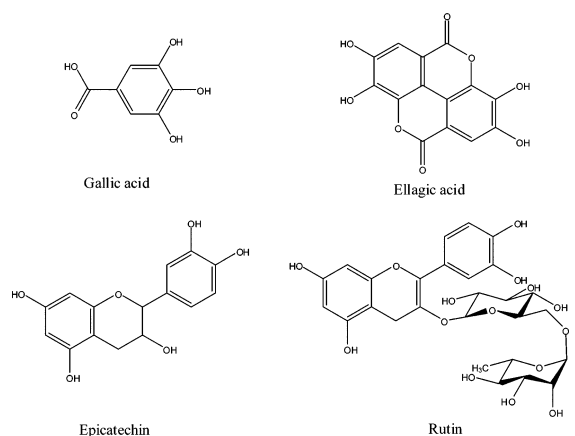


Figure 1. Chemical structures of phytoconstituents present in the *A. nilotica* extract.

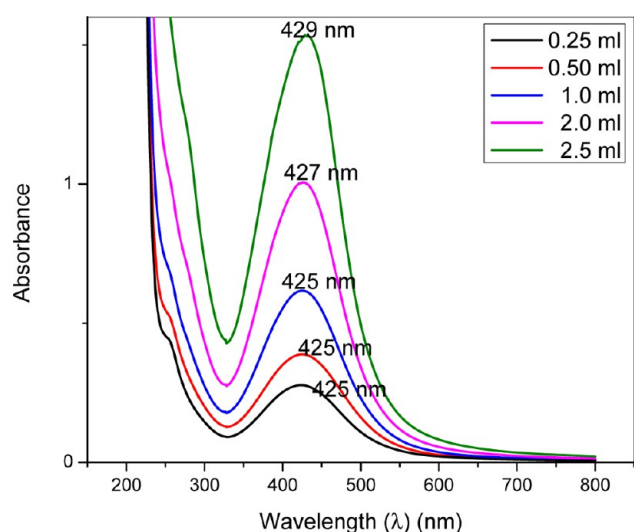


Figure 2. Effect of concentration of the *A. nilotica* pod extract on AgNPs synthesis at 6 h of reaction time.

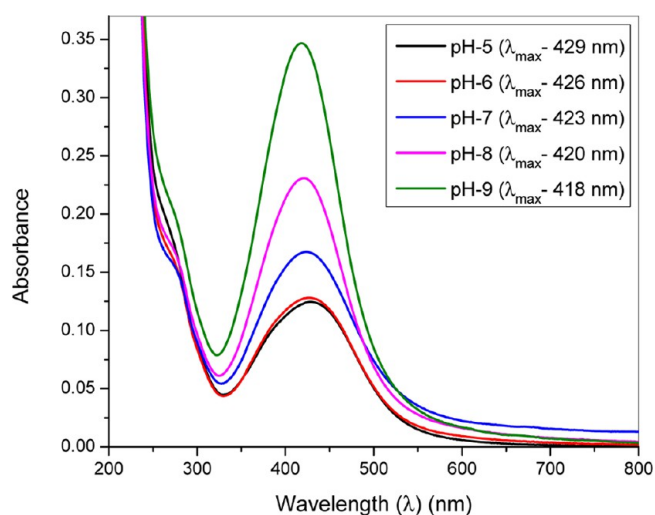


Figure 3. Effect of pH on AgNPs synthesis at 10 min of reaction time.

Synthesis of AgNPs. Synthesis of AgNPs were carried out by taking five different concentrations of the extract, viz., 0.25, 0.5, 1.0, 2.0, and 2.5 mL, and adding them separately to 24.75, 24.5, 24.0, 23, and 22.5 mL of 0.01 M AgNO_3 , respectively, (CDH Chemicals,

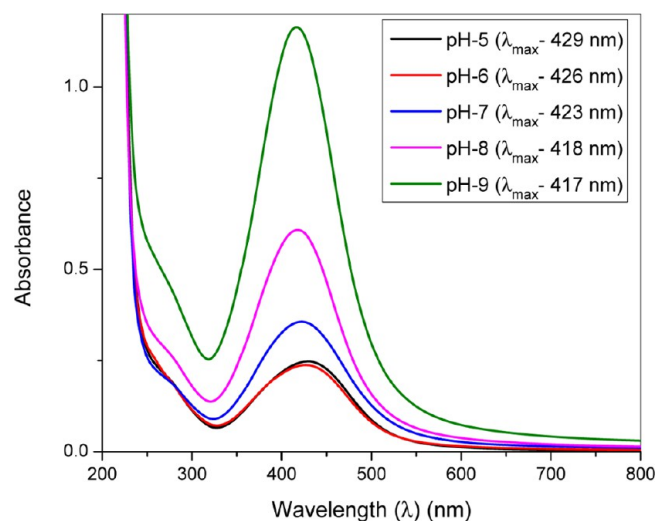


Figure 4. Effect of pH on AgNPs synthesis at 2 h of reaction time.

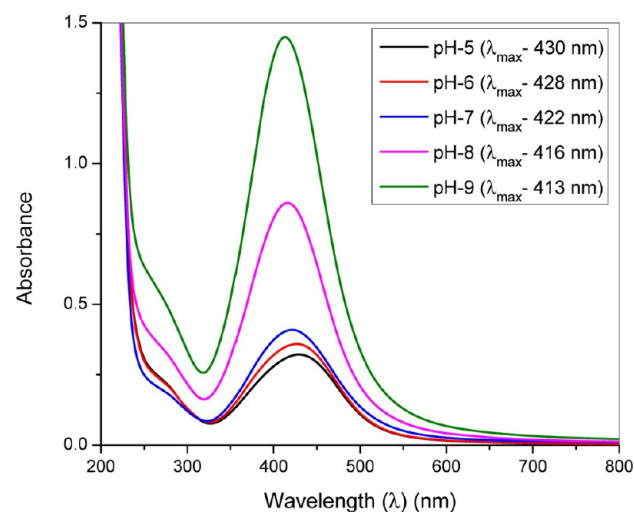


Figure 5. Effect of pH on AgNPs synthesis at 6 h of reaction time.

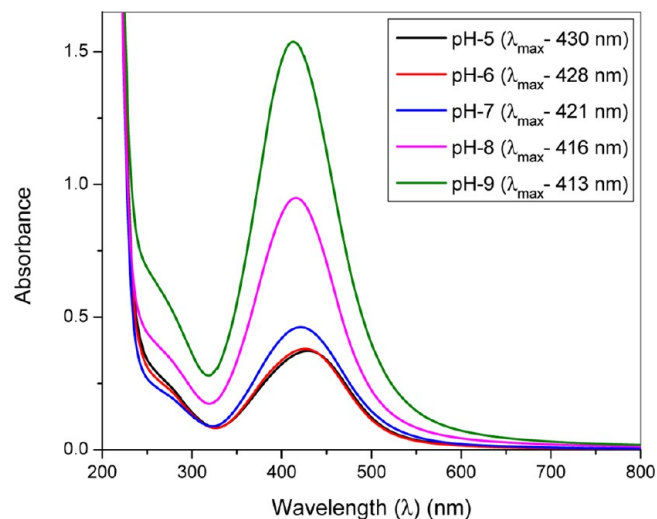


Figure 6. Effect of pH on AgNPs synthesis at 12 h of reaction time.

Mumbai, India) at room temperature. After addition of the extract, the reaction was continuously examined by visual and UV-vis spectrophotometer (PerkinElmer 35 UV-visible spectrophotometer).

The size and shape of AgNPs was mainly controlled by pH of the reaction medium. The effect of change of pH ranging from 5 to 9 on the AgNPs synthesis was studied by taking 1 mL of the extract and adding to 24 mL of 0.01 M AgNO₃ at various time intervals. The pH was varied by the addition of 0.1 M sulfuric acid in the acidic region and 0.1 M sodium hydroxide solution in the basic region. For UV–vis spectral analysis, 0.1 mL of AgNPs was taken in a cuvette and diluted by 2.9 mL of distilled water. The stable small AgNPs were chosen for further investigation and characterization.

Dynamic Light Scattering (DLS) with Zeta Potential Analysis. The stability and size distribution of AgNPs synthesized

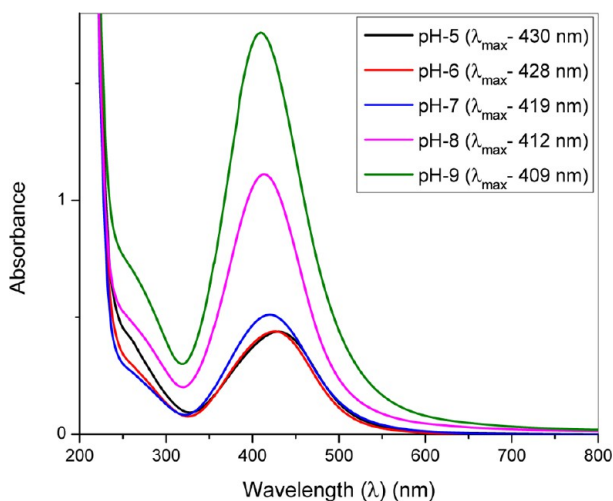


Figure 7. Effect of pH on AgNPs synthesis at 24 h of reaction time.

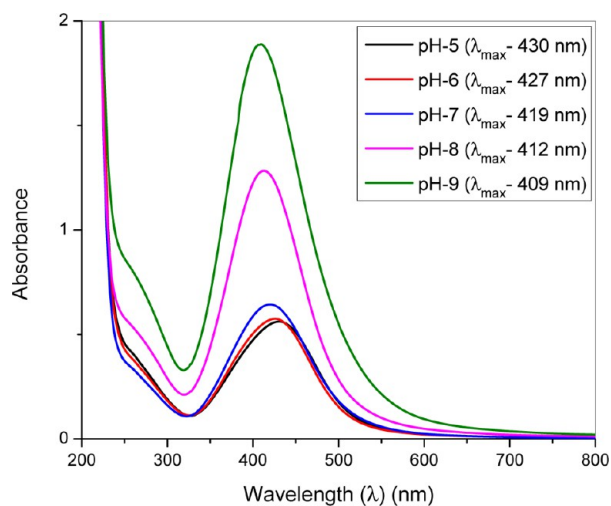


Figure 8. Effect of pH on AgNPs synthesis at 48 h of reaction time.

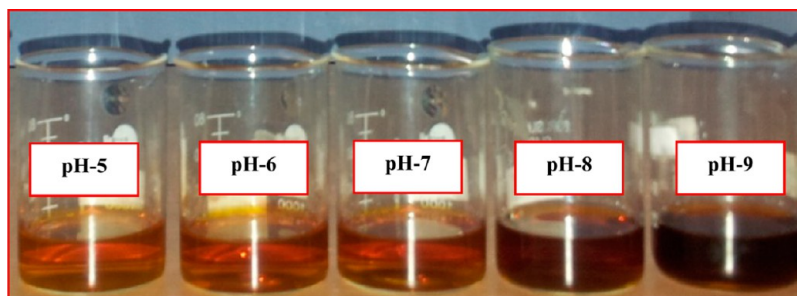


Figure 9. Visual observation of the synthesis of AgNPs at different pH ranges at 24 h of reaction time.

at pH, viz., 5, 7, and 9, were measured using Zetasizer Nano S90 (Malvern).

Characterization of Synthesized AgNPs. FT-IR Spectroscopy. The functional groups of phytoconstituents, which probably protect the AgNPs through capping, were analyzed by JASCO FT-IR 400 by mixing the dried aqueous extract and AgNPs with KBr to make the pellet for FT-IR studies.

HR-TEM with EDS Analysis. The synthesized AgNPs were washed and diluted using distilled water to fix the absorbance at 0.5 using UV–vis spectrophotometer. One drop of diluted AgNPs were drop casted onto a Cu grid carbon disc and was allowed to dry in air. After drying, the AgNPs were characterized with a JEOL JEM 2100 high resolution-transmission electron microscope operating in the range of 200 kV of acceleration. Simultaneously, the energy dispersive spectrum (EDS) was also recorded.

Electrocatalytic Activity Analysis by Cyclic Voltammetry. For investigating the electrocatalytic activity of AgNPs, the synthesized AgNPs were drop casted onto a glassy carbon electrode (3 mm diameter) and allowed to dry for 6 h. The AgNPs-modified electrode thus obtained was used to study the electrocatalytic activity by cyclic voltammetry. Simultaneously, the electrochemical response of the unmodified glassy carbon electrode and bulk metallic silver electrode (3 mm diameter) was also measured.

All the electrochemical experiments were performed using a CHI 760 D electrochemical workstation built with CHI 760 D software. The standard three electrode system was used, in which a glassy carbon electrode or silver or AgNPs-modified electrode served as a working electrode, platinum wire as a counter electrode, and saturated calomel electrode as a reference electrode. Benzyl chloride (0.001 M) was used as the electrolyte, while 0.1 M TEAP was used as supporting electrolyte and acetonitrile as a solvent. The total volume of the electrolytes was fixed as 25 mL. The potential window was fixed as -1.4 V to -0.4 V; the scan was started from negative (cathodic) potential at the scan rate of 10 mV/Sec.

RESULTS AND DISCUSSION

UV–vis Spectroscopy and DLS Studies. UV–vis spectroscopy is an indirect method to examine the formation of biogenic AgNPs from AgNO₃ solution. During the formation of AgNPs, a visible color change (from colorless to yellow) occurred. The intensity of the yellow color increased with an increase in concentration of the extract. Previous workers have reported that the formation of a yellow color and an increase in intensity of color could be due to the excitation of surface plasmon vibrations.²³ The surface plasmon resonance (SPR) is collective oscillations of the conductive electrons of AgNPs. Excitation of the surface plasmon causes strong light scattering by an electric field of the wavelength where resonance occurs. This phenomenon results in the appearance of strong SPR bands. The optical absorbance spectrum is dominated by the SPR, which shows a red shift or blue shift depending upon the particle size, shape, state of aggregation, and surrounding dielectric medium.²⁴ The increase in absorbance values (Figure 2) with

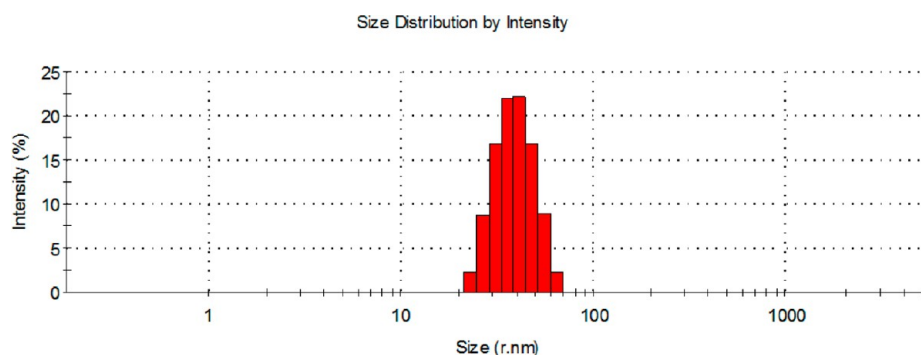


Figure 10. DLS size distribution of AgNPs at pH 9 at 24 h of reaction time.

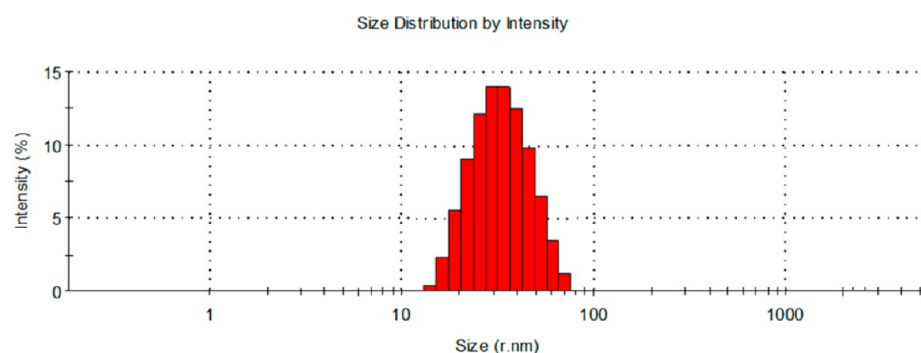


Figure 11. DLS size distribution of AgNPs at pH 7 at 24 h of reaction time.

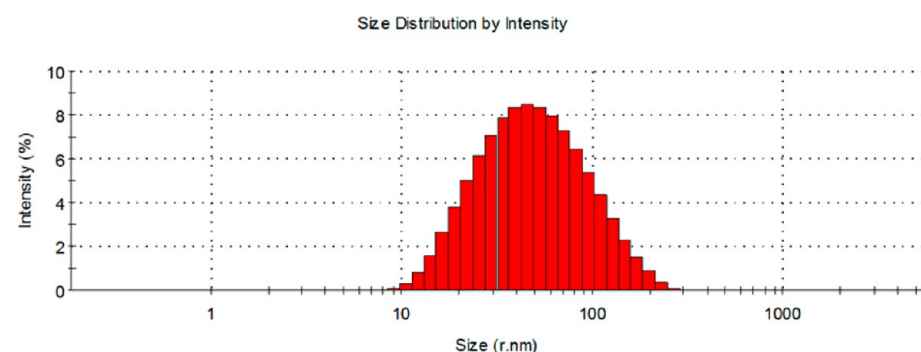


Figure 12. DLS size distribution of AgNPs at pH 5 at 24 h of reaction time.

increase in the concentration of AgNPs demonstrates higher production of AgNPs.²⁵ Stamplecoskie et al.²⁶ have reported that AgNPs, which have spherical shapes, show SPR in the region 400–440 nm. Hence, the UV studies give clues regarding the shape of AgNPs generated. Upon an increase in concentration, the SPR peak, which was observed at 425 nm, underwent a red shift indicating an increase in the particle size with an increase in the concentration of the extract. Several workers have discussed the influence of the pH of the medium over the size of the nanoparticles. In fact, size-controlled gold nanoparticles formation and size-controlled green synthesis of AgNPs have been carried out.^{27,28}

The effect of change of pH on the biosynthesis of AgNPs using *A. nilotica* extract has been studied by recording its UV–vis spectrum at different pH values, viz., 5, 6, 7, 8, and 9. In all the pH ranges, the SPR appeared between 409 and 430 nm indicating that there is no change in the shape of the nanoparticles with change in pH. However, as shown in Figures 3–8, as the pH changes from an acidic to a basic region, a hypsochromic shift was observed that indicated the reduction

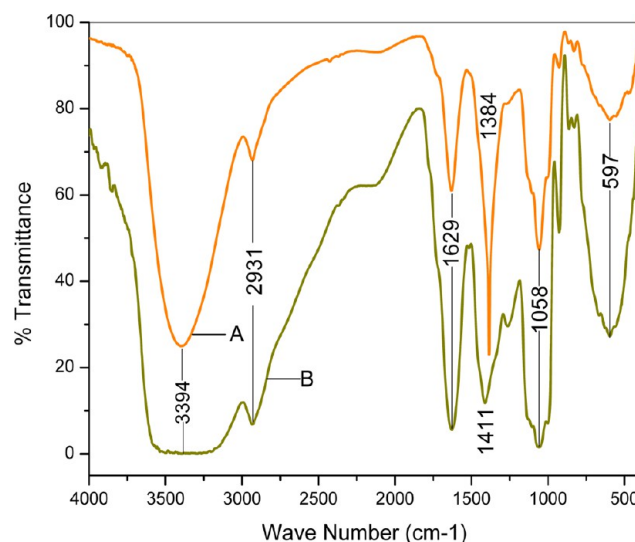


Figure 13. FT-IR spectra of *A. nilotica* pod extract (B) and synthesized AgNPs (A).

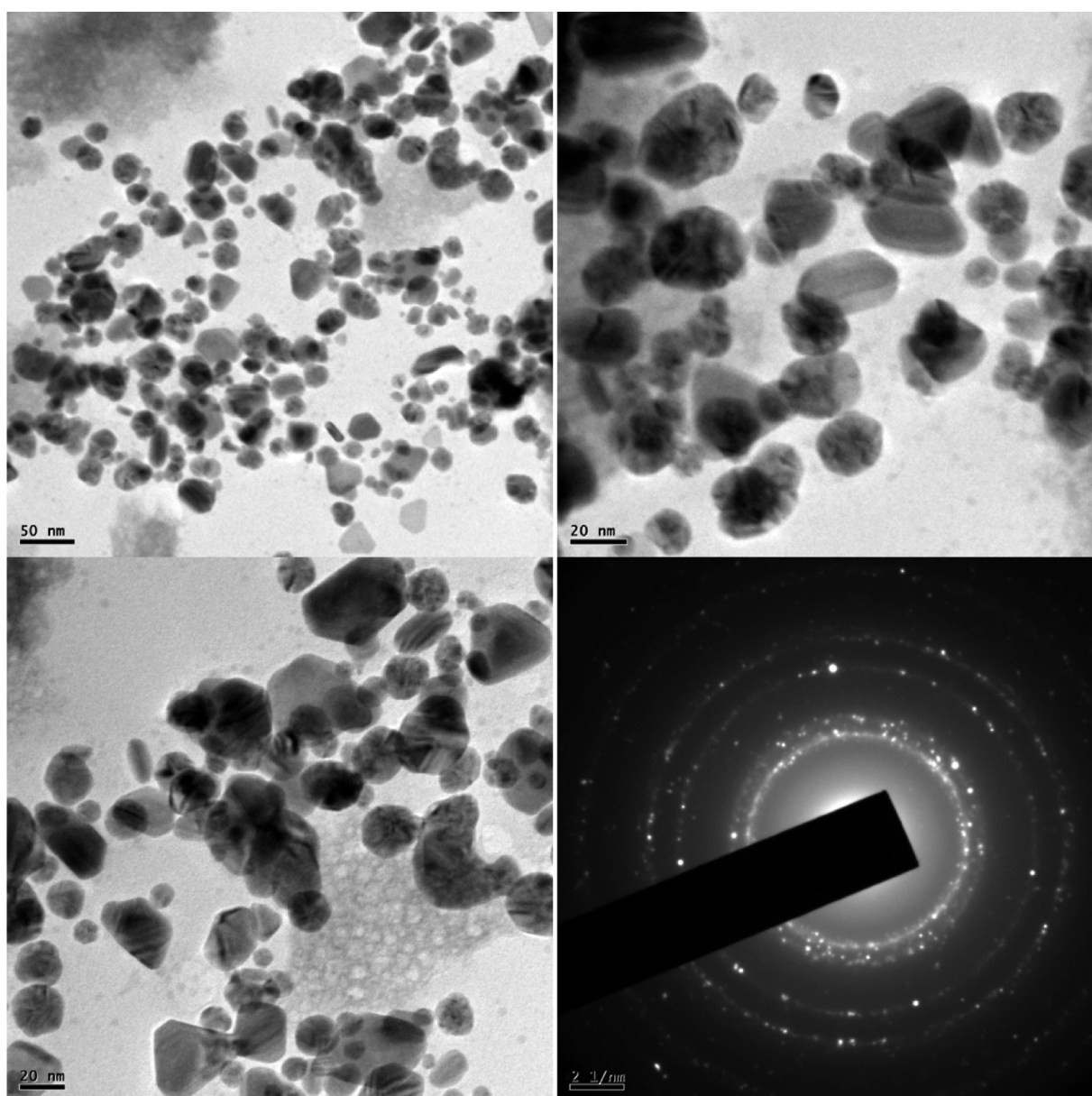


Figure 14. HR-TEM images of synthesized AgNPs at pH 7 at 24 h reaction time at different magnifications (A, B, and C) and SAED pattern of AgNPs (D).

in the size of the particles.²⁹ Hence, this study demonstrates that by changing the pH suitably, the particle size could be lowered. The effect of pH at various intervals of time also demonstrates that duration of time has little effect over the size of AgNPs. Even after 48 h, there is no aggregation of the nanoparticles as shown in Figures 3–8. The visual observation of synthesized AgNPs at 24 h of reaction time is shown in Figure 9. In other words, the study confirms the nonformation of aggregates over a longer duration of time, which vouches for the stability of AgNPs. This validates that *A. nilotica* pods are viable sources for the synthesis of nanosized silver particles.

In order to determine the particle size distribution of AgNPs in solution, DLS measurements were carried out after 24 h of reaction time at three different pH values, viz., 5, 7, and 9. The qualitative DLS size distribution image of AgNPs is shown in Figures 10–12. The average particle sizes of AgNPs in the pH 5, 7, and 9 range are 45, 29, and 20 nm, respectively. The corresponding zeta potential values are -36.2 , -52.1 , and

-51.9 mV, suggesting the high stability of AgNPs at pH 7.³⁰ The large negative potential value could be due to the capping of phytoconstituents, viz., gallic acid, ellagic acid, epicatechin, and rutin, which are present in the extract. From the results of the above study, it could be inferred that neutral pH (pH 7) is the optimum pH for the formation of highly stable AgNPs. These results agree with our earlier observation.¹⁴ The AgNPs synthesized in the pH 7 at 24 h of reaction time were further analyzed and characterized.

FT-IR Studies. FT-IR spectrum of dried aqueous extract and synthesized AgNPs obtained at optimum pH at 24 h of reaction time are shown in Figure 13. The IR-spectrum of *A. nilotica* extract showed an absorption band (broad) at 3394 cm^{-1} , which is the characteristic of $-\text{OH}$ stretching of the H-bonded phenolic group. The small sharp band appearing at 2931 cm^{-1} may be due to $-\text{CH}$ stretching of methylene group. The absorption band at 1629 cm^{-1} corresponds to the carbonyl group of carboxylic acid in the extract. The sharp bands at 1411 cm^{-1}

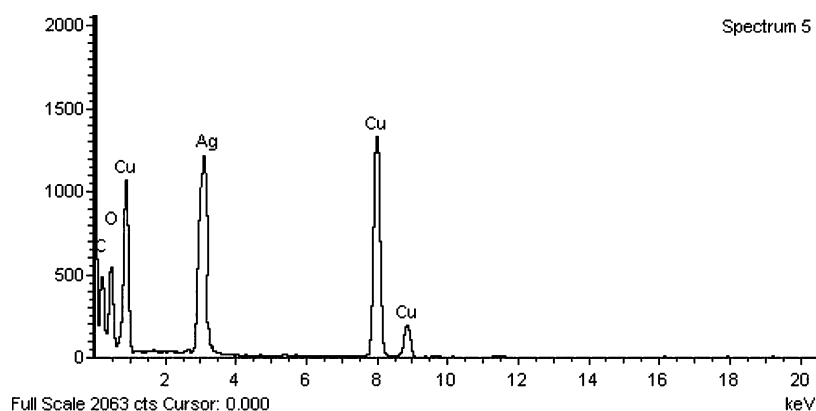


Figure 15. EDS profile of synthesized AgNPs.

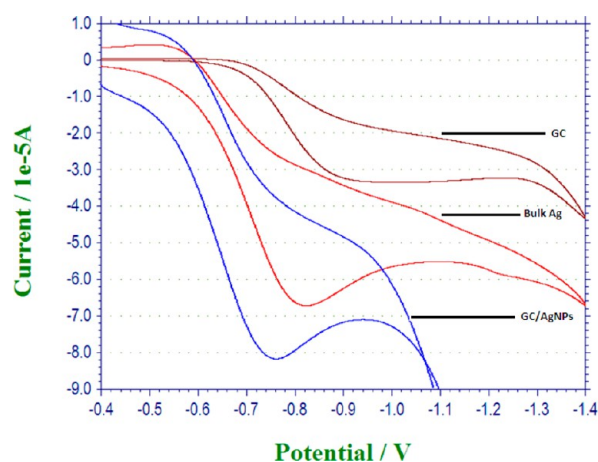


Figure 16. Cyclic voltammogram of reduction of benzyl chloride in acetonitrile +0.1 M TEAP at GC, bulk silver, and GC-modified AgNPs.

and 597 cm^{-1} indicated $-\text{OH}$ bending of the phenolic group. The band appearing at 1058 cm^{-1} could be due to the $-\text{C}-\text{O}$ stretching of phenolic acid. The absorption bands that appeared in the IR spectrum of the aqueous extract could also be seen in the synthesized AgNPs. Moreover, the sharp band appearing at 1384 cm^{-1} in the IR spectra of AgNPs is due to the presence of a nitrate ion. This suggested that the synthesized AgNPs are protected by the phytoconstituents, viz., gallic acid, ellagic acid, epicatechin, and rutin, that are present in the aqueous extract.

HR-TEM with EDS Analysis. The HR-TEM images of stable AgNPs and the SAED pattern recorded at neutral pH after 24 h of reaction time are depicted in Figure 14. From the images, it can be seen that the AgNPs are capped with phytoconstituents of the extract. Moreover, the size of the AgNPs were around 20–30 nm with distorted spherical shapes. The SAED pattern reveals that the synthesized AgNPs are crystalline (white dots in Figure 14) and mainly distorted in the (111) plane with fcc geometry. The EDS of phytocapped AgNPs is presented in Figure 15. The EDS contains the major signal of the Ag atoms, which indicated the fact AgNPs were uniformly distributed in the carbon disc. The weak signals of O and C also had appeared, which ought to have come from the phytoconstituents of the *A. nilotica* extract. The Cu peak had come from the TEM grid.

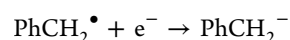
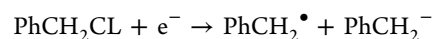
Electrocatalytic Activity Analysis. The biosynthesized stable AgNPs were tested for their efficacy in catalyzing the reduction of benzyl chloride. Apart from glassy carbon, two

types of silver electrodes were used for assessing the catalytic activity of phytosynthesized AgNPs. The cyclic voltammogram of the three electrodes are depicted in Figure 16. It is shown that a single irreversible peak was observed for all three electrodes, which is the indication of electro-reduction of benzyl chloride. The voltammetric behavior of benzyl chloride at bulk Ag is quite similar to that of glassy carbon. The results obtained from the voltammogram are shown in Table 1. A

Table 1. Voltammetric Data for Reduction of Benzyl Chloride in Acetonitrile +0.1 M TEAP at GC, Bulk Silver, and GC-Modified AgNPs

electrode	potential (V)	current $\times 10^{-5}$ A
GC	−0.81	−6.14
bulk silver	−0.78	−7.19
GC/AgNps	−0.74	−8.22

positive shift of the peak from -0.81 V to -0.78 V was observed in metallic Ag, which indicated the catalytic role of silver in reduction of benzyl chloride.³¹ The position of the peak depended heavily on the electrode material. The AgNPs-modified glassy carbon electrode showed greater catalytic activity (significant positive shift) on the reduction of benzyl chloride when compared to those of glassy carbon and metallic Ag electrode. The mechanism of the electrocatalytic reduction of benzyl chloride is depicted herein.



Isse et al.³² have shown that adsorption of both the PhCH_2Cl molecule and its reduction products play an important role in the electrocatalytic process. The biogenic AgNPs with large surface areas provide wide avenues for adsorption of both PhCH_2Cl and its reduction products, which explains its better electrocatalytic behavior than bulk Ag. Thus, extraordinary electrocatalytic effect of AgNPs is probably related to the diffusion-controlled process occurring at the surface of the nanoparticles and to the high affinity of the AgNPs with chloride ions.³³

CONCLUSIONS

The present study has demonstrated that AgNPs could be easily prepared by a green method using the aqueous extract of *A. nilotica* pods. The concentration of extract and the pH of the medium play a role in controlling the size of AgNPs. The

phytoconstituents such as gallic acid, ellagic acid, epicatechin, and rutin act as reducing agents for the synthesis of AgNPs, and the capping of AgNPs are evident from FT-IR studies. The HR-TEM images showed that the synthesized stable AgNPs are approximately 20–30 nm in size with distorted spherical shapes. The SAED pattern revealed the crystalline nature of the AgNPs. The significant positive shift in cyclic voltammogram of AgNPs compared to that of bulk Ag and glassy carbon suggested high electrocatalytic activity of synthesized AgNPs.

AUTHOR INFORMATION

Corresponding Author

*E-mail: mgsethu@gmail.com. Phone: +91 (0) 451 – 2452371. Mobile: +91-9443021565.

Notes

The authors declare no competing financial interest.

REFERENCES

- (1) Song, J. Y.; Jang, H. K.; Kim, B. S. Biological synthesis of gold nanoparticles using *Magnolia kobus* and *Diopyros kaki* leaf extracts. *Process. Biochem.* **2009**, *44* (10), 1133–1138.
- (2) Lloyd, J. R.; Byrne, J. M.; Coker, V. S. Biotechnological synthesis of functional nanomaterials. *Curr. Opin. Biotechnol.* **2011**, *22* (4), 509–515.
- (3) Sneha, K.; Sathishkumar, M.; Mao, J.; Kwak, I. S.; Yun, Y. S. *Corynebacterium glutamicum*-mediated crystallization of silver ions through sorption and reduction processes. *Chem. Eng. J.* **2010**, *162* (3), 989–996.
- (4) Jacob, J. A.; Biswas, N.; Mukherjee, T.; Kapoor, S. Effect of plant-based phenol derivatives on the formation of Cu and Ag nanoparticles. *Colloids Surf., B* **2011**, *87* (1), 49–53.
- (5) Narayanan, K. B.; Sakthivel, N. Extracellular synthesis of silver nanoparticles using the leaf extract of *Coleus amboinicus* Lour. *Mater. Res. Bull.* **2011**, *46* (10), 1708–1713.
- (6) Kumar, V. G.; Gokavaram, S. D.; Rajeswari, A.; Dhas, T. S.; Karthick, V.; Kapadia, Z.; Shrestha, T.; Barathy, I. A.; Sinha, A. R. S. Facile green synthesis of gold nanoparticles using leaf extract of antidiabetic potent *Cassia auriculata*. *Colloids Surf., B* **2011**, *87* (1), 159–163.
- (7) Horwat, D.; Zakharov, D. I.; Endrino, J. L.; Soldera, F.; Anders, A.; Migot, S.; Karoum, R.; Vernoux, Ph.; Pierson, J. F. Chemistry, phase formation, and catalytic activity of thin palladium-containing oxide films synthesized by plasma-assisted physical vapor deposition. *Surf. Coat. Technol.* **2011**, *205* (2), S171–S177.
- (8) Dillon, A. C.; Mahan, A. H.; Deshpande, R.; Alleman, J. L.; Blackburn, J. L.; Parillia, P. A.; Heben, M. J.; Engtrakul, C.; Gilbert, K. E. H.; Jones, K. M.; To, R.; Lee, S.-H.; Lehman, J. H. Hot-wire chemical vapor synthesis for a variety of nano-materials with novel applications. *Thin Solid Films* **2006**, *501* (1–2), 5.
- (9) Sobhani, M.; Rezaie, H. R.; Naghizadeh, R. Sol–gel synthesis of aluminum titanate (Al_2TiO_5) nano-particles. *J. Mater. Process. Technol.* **2008**, *206* (1–3), 282–285.
- (10) Nadagouda, M. N.; Speth, T. F.; Varma, R. S. Microwave-assisted green synthesis of silver nanostructures. *Acc. Chem. Res.* **2011**, *44* (7), 469–478.
- (11) Wani, I. A.; Ganguly, A.; Ahmed, J.; Ahmad, T. Silver nanoparticles: Ultrasonic wave assisted synthesis, optical characterization and surface area studies. *Mater. Lett.* **2011**, *65* (3), 520–522.
- (12) Starowicz, M.; Stypula, B.; Banas, J. Electrochemical synthesis of silver nanoparticles. *Electrochem. Commun.* **2006**, *8* (2), 227–230.
- (13) Kima, K. D.; Hanb, D. N.; Kim, H. T. Optimization of experimental conditions based on the Taguchi robust design for the formation of nano-sized silver particles by chemical reduction method. *Chem. Eng. J.* **2004**, *104* (1–3), 55–61.
- (14) Edison, T. J. I.; Sethuraman, M. G. Instant green synthesis of silver nanoparticles using *Terminalia chebula* fruit extract and evaluation of their catalytic activity on reduction of methylene blue. *Process. Biochem.* **2012**, *47* (9), 1351–1357.
- (15) Edison, T. J. I.; Sethuraman, M. G. Biogenic robust synthesis of silver nanoparticles using *Punica granatum* peel and its application as a green catalyst for the reduction of an anthropogenic pollutant 4-nitrophenol. *Spectrochim. Acta, Part A* **2013**, *104* (1), 262–264.
- (16) Merin, D. D.; Prakash, S.; Bhimba, B. V. Antibacterial screening of silver nanoparticles synthesized by marine micro algae. *Asian Pac. J. Trop. Med.* **2010**, *3* (10), 797–799.
- (17) Gajbhiye, M.; Kesharwani, J.; Ingle, A.; Gade, A.; Rai, M. Fungus-mediated synthesis of silver nanoparticles and their activity against pathogenic fungi in combination with fluconazole. *Nanomed.: Nanotechnol. Bio. Med.* **2009**, *5* (4), 382–386.
- (18) Jaidev, L. R.; Narasimha, G. Fungal mediated biosynthesis of silver nanoparticles, characterization and antimicrobial activity. *Colloids Surf., B* **2010**, *81* (2), 430–433.
- (19) Sadowski, Z.; Maliszewska, I. H.; Grochowalska, B.; Polowczyk, I.; Kozlecki, T. Synthesis of silver nanoparticles using microorganisms. *Mater. Sci–Pol.* **2008**, *26* (2), 419.
- (20) Nadagouda, M. N.; Castle, A. B.; Murdock, R. C.; Hussain, S. M.; Varma, R. S. In vitro biocompatibility of nanoscale zerovalent iron particles (NZVI) synthesized using tea polyphenols. *Green Chem.* **2010**, *12*, 114–122.
- (21) Nadagouda, M. N.; Varma, R. S. Green synthesis of silver and palladium nanoparticles at room temperature using coffee and tea extract. *Green Chem.* **2008**, *10*, 859–862.
- (22) Singh, B. N.; Singh, B. R.; Singh, R. L.; Prakash, D.; Sarma, B. K.; Singh, H. B. Antioxidant and anti-quorum sensing activities of green pod of *Acacia nilotica* L. *Food Chem. Toxicol.* **2009**, *47* (4), 778–786.
- (23) Rai, A.; Singh, A.; Ahmad, A.; Sastry, M. Role of halide ions and temperature on the morphology of biologically synthesized gold nanotriangles. *Langmuir* **2006**, *22* (2), 736–741.
- (24) Tripathy, A.; Raichur, A. M.; Chandrasekaran, N.; Prathna, T. C.; Mukherjee, A. Process variables in biomimetic synthesis of silver nanoparticles by aqueous extract of *Azadirachta indica* (Neem) leaves. *J. Nanopart. Res.* **2012**, *12*, 237–246.
- (25) Sathishkumar, M.; Sneha, K.; Won, S. W.; Cho, C.-W.; Kim, S.; Yun, Y.-S. *Cinnamomum zeylanicum* bark extract and powder mediated green synthesis of nano-crystalline silver particles and its bactericidal activity. *Colloids Surf., B* **2009**, *73* (2), 332–338.
- (26) Stampelcoskie, K. G.; Scaiano, J. C. Light emitting diode irradiation can control the morphology and optical properties of silver nanoparticles. *J. Am. Chem. Soc.* **2010**, *132* (6), 1825–1827.
- (27) Huang, X.; Wu, H.; Liao, X.; Shi, B. One-step, size-controlled synthesis of gold nanoparticles at room temperature using plant tannin. *Green Chem.* **2010**, *12*, 395–399.
- (28) Kora, A. J.; Beedu, S. R.; Jayaraman, A. Size-controlled green synthesis of silver nanoparticles mediated by gum ghatti (*Anogeissus latifolia*) and its biological activity. *Org. Med. Chem. Lett.* **2012**, *2*, 17.
- (29) Amendola, V.; Meneghetti, M. Size evaluation of gold nanoparticles by UV–vis spectroscopy. *J. Phys. Chem. C* **2009**, *113* (11), 4277–4285.
- (30) Rao, Y. S.; Kotakadi, V. S.; Prasad, T. N. V. K. V.; Reddy, A. V.; Gopal, D. V. R. S. Green synthesis and spectral characterization of silver nanoparticles from Lakshmi tulasi (*Ocimum sanctum*) leaf extract. *Spectrochim. Acta, Part A* **2013**, *103* (15), 156–159.
- (31) Maiyalagan, T. Synthesis, characterization and electrocatalytic activity of silver nanorods towards the reduction of benzyl chloride. *Appl. Catal., A* **2008**, *340* (2), 191–195.
- (32) Isse, A. A.; Giusti, A. D.; Gennaro, A.; Falciola, L.; Mussini, P. R. Electrochemical reduction of benzyl halides at a silver electrode. *Electrochim. Acta* **2006**, *51* (23), 4956–4964.
- (33) Bellomunno, C.; Bonanomi, D.; Falciola, L.; Longhi, M.; Mussini, P. R.; Doubova, L. M.; Silvestro, G. D. Building up an electrocatalytic activity scale of cathode materials for organic halide reductions. *Electrochim. Acta* **2005**, *50* (11), 2331–2341.